Available online at www.sciencedirect.com
ScienceDirect
Physica E 40 (2008) 2481–2484
PHYSICA E
www.elsevier.com/locate/physe

Unipolar rectifying silicon nanowires—TCAD study

K. Fobelets[a,*], J.E. Velazquez-Perez[b]

[a]Department of Electrical and Electronic Engineering, Imperial College London, Exhibition Road, South Kingston, London SW7 2BT, UK
[b]Departamento de Física Aplicada, Universidad de Salamanca, Edificio Trilingue, Pza de la Merced s/n, E-37008 Salamanca, Spain

Available online 20 September 2007

Abstract

Due to the large surface to volume ratio in nanowires, small changes in surface condition result in large changes in current–voltage characteristics. As a consequence, the overlap of the end-wire contact with the oxide-covered surface along the length of the nanowire can have a significant effect on the current–voltage characteristics of the wire. We present TCAD studies of this effect. One of the contacts at the end of the wire envelops a part of the surface along the length of the oxide-covered nanowire, resulting in a partial gating of the wire by the voltage applied to the Ohmic contact. This gating causes rectifying behaviour in the unipolar nanowire, creating a conducting surface channel in forward bias and space-charge-limited current in reverse bias. TCAD studies show that the length of contact overlap relative to the length of the nanowire influences the off-current to a large extent, dramatically decreasing the off-current with increasing overlap. TCAD results of the influence of wire diameter, length, and workfunction on the rectifying behaviour of the unipolar nanowire are also presented.

PACS: 81.07.−b; 73.63.−b; 78.67.−n

Keywords: Nanowires; TCAD; Rectification

1. Introduction

Over the last couple of years, interest in nanowires (NWs) has dramatically increased due to the downscaling effort in semiconductor technology. The resulting small structures such as NWs, whiskers, and dots are governed by different physical principles than their bulk counterparts as the surface plays an increasingly important role. As a consequence, what happens on the surface will influence the behaviour of the nanodevices substantially. Benefits of the NW technology have been demonstrated in a variety of applications such as thermoelectricity [1], sensing [2], field effect transistors [3,4], optics [5], etc. A review on the topic of electronic and optical NWs can be found in e.g. Ref. [6]. Notwithstanding these successes, some basic questions remain, such as stochastic changes in the local doping density and contacting issues.

In this manuscript, we investigate the influence of the overlap of the end contact over the surface along the length of the oxide-coated NW. We find that this overlap causes rectifying behaviour without the need for doping. This result can be seen as a potential novel application, where rectifying behaviour is established while circumventing the need for doping and thus alleviating the stochastic changes of the doping density. On the other hand, it also shows that the overlap of the Ohmic contact with a part of the oxide-coated surface along its length determines the characteristics of the wire, making it rectifying rather than linear.

The NW structure is given in Fig. 1. MOSFET terminology is used to name the contacts as the structure shows some similarity with wrap-around gate MOSFETs [7]. It consists of an Ohmic contact, S at one side of the wire and a combined Ohmic/gate contact, D at the other side. Contact D is special in the sense that the same voltage that makes the charged carriers drift also gates a specific part of the wire, depleting or enhancing it of mobile carriers. The electric field across the oxide along the length of the wire will cause a variation of the depletion/

*Corresponding author. Tel.: +44 2075946236; fax: +44 2075946308.
E-mail address: k.fobelets@ic.ac.uk (K. Fobelets).

1386-9477/$ - see front matter © 2007 Elsevier B.V. All rights reserved.
doi:10.1016/j.physe.2007.09.033

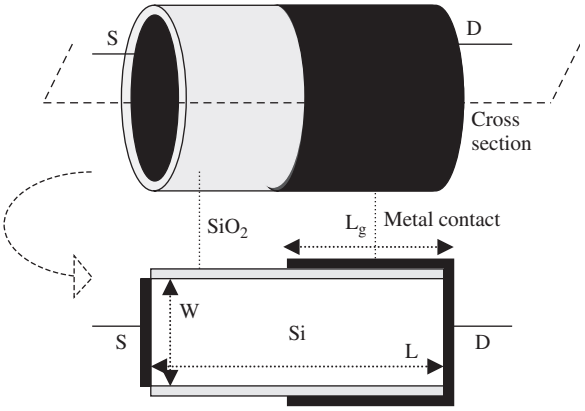

Fig. 1. Schematic drawing of a unipolar rectifying semiconductor NW. Top: 3D view and bottom: 2D cross section through the middle of the cylinder (dashed line). Colour coding—grey: SiO_2, white: Si, and black: contact.

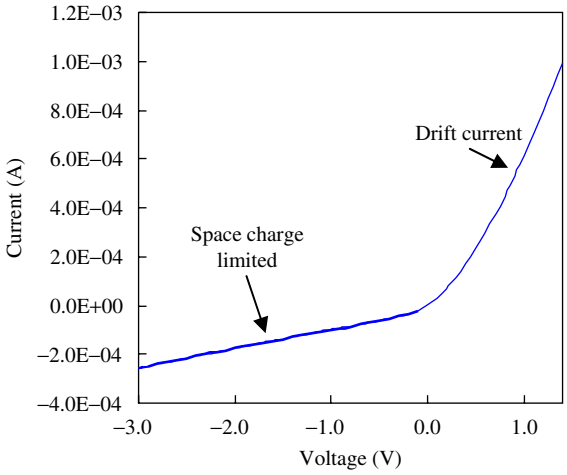

Fig. 2. Current–voltage characteristic of a unipolar NW with contact overlap.

accumulation region that modulates the flow of the carriers. The parameters of the NW are: diameter W, length L, and contact overlap length L_g. The voltage is applied to D and S is grounded.

The main differences between the wrap-around MOSFET and the NW are that the channel in the NW carries the same doping type as the contacts, the distance between S and D is relatively large and not equal to the gated length, and the applied voltage is varied in both bias directions. In contrast to the NW, MOSFETs function in inversion between S and D and when diodes connected have a quadratic IV characteristic.

For the 2D modelling, MEDICI from Synopsis [8] is used. Changing modelling parameters such as drift-diffusion/hydrodynamic model, mobility models (surface scattering or not), and end contact boundary condition (neutral/workfunction/insertion of highly doped contact regions) give the same qualitative results for the NWs of 100 and 50 nm diameter used in this work. Quantitatively, the hydrodynamic model gives lower current amplitudes, while end contact choice and scattering have a minor effect.

2. Functioning of the unipolar rectifying nanowire

Here we briefly discuss the physics behind the rectification character of the unipolar NW. The material and geometrical parameters of the wire used in the calculation are: $W = 100\,\text{nm}$, $L = 200\,\text{nm}$, $L_g = 100\,\text{nm}$, oxide thickness $t_{ox} = 2\,\text{nm}$, n-type background doping of the wire $N_D = 10^{16}\,\text{cm}^{-3}$ and workfunction of the contacts $\phi = 4.32\,\text{eV}$. In Fig. 2, the non-linear current–voltage characteristic is given. The on-current at 1 V is 6 times larger than at −1 V. Since the drain contact overlaps the length of the NW partially, this results in a gating effect along the overlap length. The voltage on the drain will thus cause drift and gating simultaneously. This results in a varying degree of depletion/inversion of carriers between S and D.

The NW characteristic is similar to that of a diode with current limitation in reverse bias. However, in forward bias the currents in the NW are not exponential but quasi-linear. The use of a unipolar NW instead of a pn-diode has the advantage of avoiding the excess minority carrier storage delay time when switching. An estimation of the RC time constant of the NW based on oxide capacitance $C_{ox} = \varepsilon_0\varepsilon_{ox}(\pi W L_g)/t_{ox}$ and differential resistance

$$R = \left.\frac{dV}{dI}\right|_{V=1\,\text{V}}$$

gives a value of $RC \approx 10^{-11}\,\text{s}$.

In Fig. 3, the carrier concentration is plotted as a function of wire width at two different positions along its length, one at a position outside (50 nm) and the other through (150 nm) the gated region.

For negative or reverse bias the surface of the wire is depleted of mobile carriers causing space-charge-limited currents. This picture is reversed for positive bias as strong accumulation occurs in the gated region and thus drift currents happen in the accumulated surface channel region. These variations in carrier concentration near the surface of the wire, imposed by the applied drift voltage (drain), are similar to graded junctions. Interestingly, the stray electric field on the overlap region causes slight variations in the surface carrier concentration in the un-gated region. In the middle of the 100 nm wire, the gate voltage has limited influence. Decreasing the wire diameter will result in a better control of the carrier concentration through the width of the channel. This is similar to modelling results on double-gated finFETs.

3. Influence of device parameters

In this section, results of the influence of the NW diameter W, length L, contact overlap length L_g, and contact workfunction ϕ are given. In Fig. 4 we show the influence of L_g and W. The other parameters are

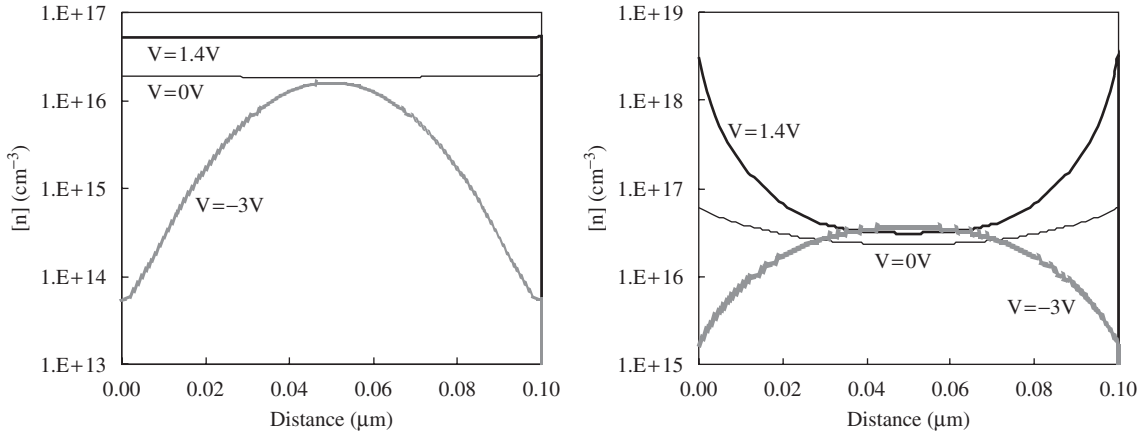

Fig. 3. Carrier concentration as a function of the distance through the width of the wire at 50 nm (left) and 150 nm (right) from the source, S for three different drain voltages, $V = -3$, 0 and 1.4 V.

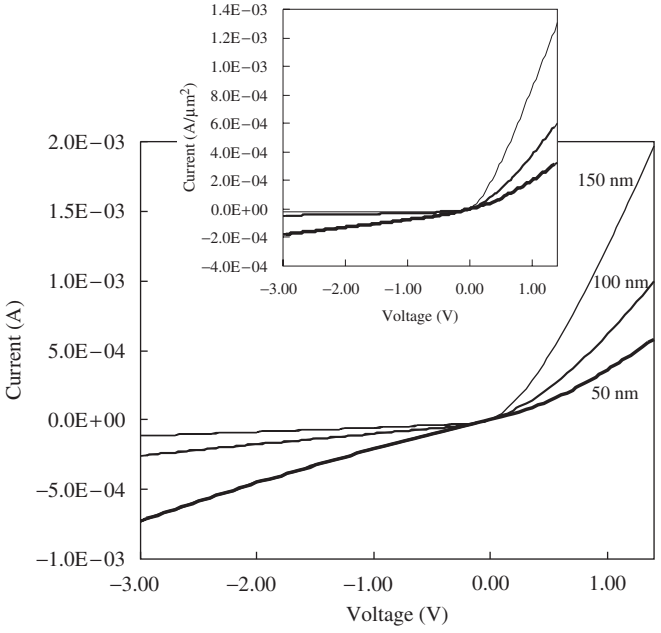

Fig. 4. Current–voltage characteristic of a NW ($W = 100$ nm) for different overlap lengths L_g: 50, 100 and 150 nm. Inset: wire of $W = 50$ nm (same legend).

$L = 200$ nm, $t_{ox} = 2$ nm, $N_D = 10^{16}$ cm^{-3}, $\phi = 4.32$ V. L_g is 50, 100, and 150 nm for two different widths, 100 and 50 nm.

As the overlap length changes, both the on- and off-currents alter. Increasing L_g lowers the off-current and increases the on-current. Thus, increasing the length of the "gate" results in better rectifying characteristics of the NW. Or, alternatively, variations in the overlap of the Ohmic contact and the oxide-covered length of the wire result in dramatic changes in the current–voltage characteristics. Thus, care must be taken in contacting NWs to avoid this feature if unwanted.

This result is not surprising; when the overlap length increases, it will deplete the mobile carriers over a longer length, and thus the wire becomes more resistive overall and current decreases. In case of forward bias, more carriers are accumulated over the length of the channel, thus increasing the current. The results for the 50 nm wire are qualitatively the same, but the control of the "gate" is more effective, giving lower off-currents.

In Fig. 5, the dependency on the length of the wire is given. The wire parameters are $L = 200$ and 700 nm with $L_g = 1/2L$ in, (a) and $L_g = L$ in (b). The rectifying character remains, but for longer wires with the same geometrical parameters the currents are lower due to the higher resistance of the un-gated regions which cause a decrease in effective drift voltage.

The influence of the workfunction ϕ of the contacts is also studied. The parameters are $W = 100$ nm, $t_{ox} = 2$ nm, $L = 700$ nm, $\phi = 4.32$ V, and $L_g = 1/2L$. The results are given in Fig. 6. Relatively large changes can be seen in the reverse bias current of the NW as a function of workfunction as a consequence of the band bending imposed by the workfunction difference between "gate" metal and semiconductor.

Thus, the rectifying behaviour in an overlap situation between Ohmic contact and an oxide-coated wire surface will be dependent on the metal used. This result can also be exploited for sensor applications similar to ISFET technology [9], but in the NW case we have a device with only two contacts.

In the ISFET, the gate potential is changed due to the ion concentration in the electrolyte surrounding the gate. The change in gate potential changes the threshold voltage of the FET and thus changes the source to drain current.

Following the reasoning presented in Ref. [10], the threshold voltage of the ISFET, V_{th}^{ISFET}, can be written as

$$V_{th}^{ISFET} = V_{th}^{MOSFET} + \psi_S(\mathrm{pH}) + c_0,$$

where

- V_{th}^{MOSFET} is the threshold voltage of the classical semiconductor MOSFET [11];

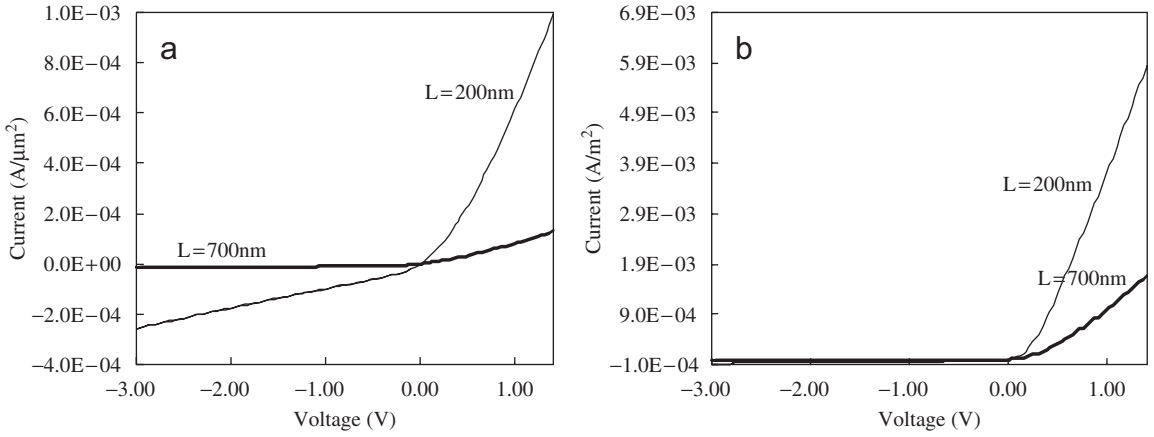

Fig. 5. Influence of the length of the wire on the current–voltage characteristics. $W = 100$ nm, $t_{ox} = 2$ nm, $\phi = 4.32$ V, $L = 200$, and 700 nm: (a) $L_g = 1/2L$, (b) $L_g = L$.

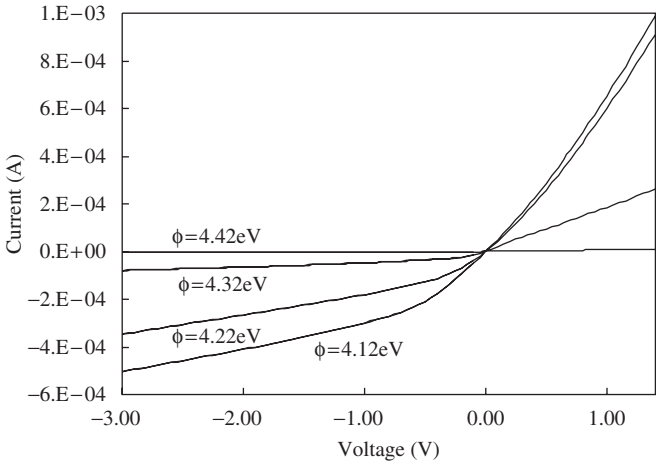

Fig. 6. Influence of workfunction difference on the current–voltage characteristics of a NW with $W = 100$ nm, $t_{ox} = 2$ nm, 700 nm, and $L_g = 1/2L$.

- ψ_S(pH) is the shift in threshold voltage due to the pH of the electrolyte; and
- c_0 is a constant taking into account other non-ion concentration-related threshold voltage shifts.

The function ψ_S(pH) is dependent on the chosen ion-sensitive oxide material of the ISFET [9]. The sensitivity is given by the slope of ψ_S(pH). In TCAD, we can model ψ_S(pH) as a variation of the workfunction difference between the semiconductor ϕ_s and the gate metal ϕ_m, because $\phi_m - \phi_s$ occurs as a term in V_{th}^{MOSFET} [11]. Changing this term within the range of the ψ_S(pH) will model the threshold voltage shift due to the pH of the electrolyte. Although the unipolar NW is not a FET, $\phi_m - \phi_s$ in the overlap region will have similar outcomes (see Fig. 6). Typical sensitivities of ISFETs lie in the range of 40–60 mV/pH. This means that a pH change of 1 would result in a threshold voltage shift of 40–60 mV and thus in a workfunction difference of 40–60 mV. As a consequences, when the NW is dipped with the drain side in the electrolyte to a certain depth more than $L/2$, it can function as a sensor. At constant voltage in reverse bias, the current will change according to the workfunction difference and thus pH of the analyte.

4. Conclusion

We presented TCAD results on the influence of an ohmic contact that overlaps a fractional length of an oxide-coated Si nanowire. This overlap causes a gating effect by the Ohmic contact voltage. As a result, the characteristics of the nanowire will be rectifying. The amount of rectification generated is dependent on the length of the contact overlap and the workfunction of the contact metal. This implies that care should be taken when contacting nanowires as contact overlaps can cause drastic changes in the current–voltage characteristics. On the other hand, this feature can be exploited as a unipolar nanowire-rectifying device (diode) or as a two-contact unipolar nanowire pH sensor.

References

[1] Y. Zhang, J. Christofferson, A. Shakouri, D.Y. Li, A. Majumdar, Y.Y. Wu, R. Fan, P.D. Yang, IEEE Trans. Nanotechnol 5 (1) (2006) 67.
[2] A.K. Wanekaya, W. Chen, N.V. Myung, A. Mulchandani, Electroanalysis 18 (6) (2006) 533.
[3] A. Javey, S. Nam, R.S. Friedman, H. Yan, C.M. Nano, Lett. 7 (3) (2007) 773.
[4] V. Schmidt, H. Riel, S. Senz, S. Karg, W. Riess, U. Gosele, Small 2 (1) (2006) 85.
[5] R. Agarwal, C.M. Lieber, Appl. Phys. A 85 (3) (2006) 209.
[6] Y. Fi, F. Qian, J. Xiang, C.M. Lieber, Mat Today 9 (10) (2006) 18.
[7] E. Leobandung, J. Gu, L. Guo, S.Y. Chou, J. Vac. Sci. Technol B 15 (6) (1997) 2791.
[8] 〈www.synopsys.com〉.
[9] P. Bergveld, IEEE Trans. Biomed. Engr. BME- 19 (1972) 342.
[10] M. Janicki, M. Daniel, M. Szermer, A. Napieralski, Microelecton J 35 (2004) 831.
[11] M.S. Shur, Physics of semiconductor devices, Prentice Hall series Solid State Physical Electronics Prentice-Hall, Englewood Cliffs, NJ.